APPLICATION OF ULTRASONIC POD MODELS

T. A. Gray, F. Amin, and R. B. Thompson

Center for Nondestructive Evaluation
Iowa State University
Ames, IA 50011

INTRODUCTION

The ability to quantify the reliability of nondestructive evaluation (NDE) inspection techniques is required to integrate inspectability into the component design process. Inspectability is typically evaluated on the basis of the design engineer's experience and knowledge of NDE. While this approach can yield adequate designs with regard to inspection reliability, the potential for uninspectability remains. There is also the possibility that the designer's knowledge of the reliability of NDE techniques may be limited to "standard" approaches which may be be inadequate for new component geometries or materials. This could lead the design engineer to imagine that a given component is inadequately inspectable and to redesign the part when the correct solution is either to modify the inspection protocol or to select a different technique. Alternatively, models which predict inspection reliability could be used to weigh the trade-offs and risks associated with selection among candidate NDE techniques to be applied to inspection of a given component design and to identify NDE system configurations for optimal reliability. This approach is, in fact, a key feature of the Unified Life Cycle Engineering concept currently being developed by the Air Force[1].

Ultrasonic inspection is one NDE discipline which has achieved sufficient technical maturity to allow such application, although significant progress is being made in other arenas, e.g., x-ray radiography and eddy current modeling. In ultrasonics, a computer model has been developed which can simulate signals that would be obtained in scanned ultrasonic inspections of gas turbine engines components[2,3], and can estimate the probability of detection (POD) of both crack-like and volumetric defects[4,5]. This model explicitly incorporates the features of the inspection system, the component design, and the critical defects. The POD of critical defects can thus be predicted as functions of both the inspection protocol and the design parameters. In this paper, we will review the ultrasonic POD model and illustrate its utility via simulations to address the evaluation of trade-offs of NDE system selection for inspection of a specific component design.

REVIEW OF POD MODEL

The basis of the computer model for determining ultrasonic POD is a model for predicting the signals which would be measured in a scanned inspection of a complex shaped component. The analytical framework is an electromechanical reciprocity integral[6] that predicts the change in electrical power radiating into a coaxial line from a receiving ultrasonic transducer due to the presence of a scatterer. Various analytical models

have been incorporated into this integral to predict the fields produced by transducer; the modification, including mode conversion, of those fields induced by transmission through a curved liquid-solid interface, such as would be encountered in an immersion test; the propagation of those fields in an isotropic, attenuative, elastic medium; the elastic wave scattering from a defect in the bulk of the material; and the detection of the fields by a receiving probe. Recent reports[2,3,7] have described this measurement model, illustrated its ability to predict waveforms from spherical and crack-like defects, and compared the predictions to actual experimental signals.

A recent addition to the measurement model software is a scattering model for volumetric defects based upon the Kirchhoff approximation[9]. This approximation has been implemented for both longitudinal and shear wave backscatter from ellipsoidal voids and inclusions. The Kirchhoff approximation correctly predicts the leading edge response (front-surface reflection) from a volumetric scatterer but does not include the scattering events from later time (for example, due to focusing and reverberations of ultrasonic waves inside an inclusion). For voids, this front-surface contribution dominates the scattered signals[10]; the later events arise from a mode converted "creeping wave" which travels around the periphery of the scatterer and re-radiates as it travels. Thus, the Kirchhoff approximation is quite good for voids, since the leading edge contribution is the largest signal feature. For inclusions, the later arriving components of the scattered waves, e.g. induced by reverberations inside the scatterer, can be considerably larger than the front-surface reflection. (See, e.g., Fig. 6 in Ref. 11). In such cases, the Kirchhoff approximation will systematically underestimate the signal from an inclusion.

An extension of the modeling work for application to reliability of ultrasonic NDE, which has also been described in past reports[4,5,7], is the incorporation of the measurement model into a model for predicting the POD of flaws. This development has been devoted to simulation of the "standard" practice of threshold detection of the video envelope of scattered signals from defects obtained in automated scans of components. The approach assumes a Rayleigh probability distribution for noise and a Rician distribution for signals in the presence of such noise[8]. (The technique is similar to analysis of the probability of detection of radar signals). To apply this method, the measurement model described above is used to predict the video signal from a given defect with a specified position relative to the inspection scan lines and orientation relative to the component surface. The amplitude of this video signal defines a "mean" of the Rician distribution whose "variance" is defined by the assumed noise distribution. The probability that the given defect's signal plus noise amplitude will exceed a threshold amplitude can then be determined by a one-tailed integration of the Rician distribution function. The position and orientation of a flaw are, however, random variables. Thus, the threshold exceedance probability for the signal from a flaw with a specific position and orientation must be integrated with respect to the probability distribution functions of those random variables in order to compute the POD for all flaws of the same size but arbitrary position and orientation. Preliminary experimental tests of the POD model for crack-like defects in parts with simple shapes and for high signal-to-noise (S/N) environments have been quite favorable[4,5,7].

SIMULATION OF NDE SYSTEM TRADE-OFF RISKS

One application of the ability to predict NDE reliability, i.e. POD, is the assessment of the risks associated with trade-offs between competing NDE inspection techniques for flaw detection in a specified component. This would be applicable, for example, in selecting between ultrasonic versus eddy current inspection for near-surface defects or between ultrasonic versus x-ray radiography for bulk flaws. Application of POD modeling to trade-off analysis requires that the given NDE technique be optimized relative to the component geometry, material, etc., in order that the analysis be meaningful. The meaning of "optimal" in this context is dependent upon the specific

economic or other liability factors particular to the application, however. For example, one NDE system and/or configuration may exhibit high detection sensitivity to flaws which are smaller than the critical defect size. This could lead to a low false acceptance (FA) rate of flawed components but a high false rejection (FR) rate of parts containing defects which do not significantly affect the performance characteristics of the component. A different configuration or system, on the other hand, could significantly reduce the FR errors but increase the FA rate. Either of these two scenarios may be acceptable under certain circumstances - e.g., rejection of some good parts may be acceptable when component failure results in loss of life or when the price per piece is small, while acceptance of some flawed parts may be acceptable when failure is not life-threatening but components are expensive to manufacture or replace. However, derivation of a "cost model" for evaluation of these economic factors is beyond the scope of this report.

Primary attention in the following analysis will be directed toward illustrating the utility of the POD model for providing the NDE reliability information required to assess the inspection system trade-off risks. In addition, since an adequate capability does not yet exist for simulating POD for NDE techniques other than ultrasonics, we will illustrate only the extraction of NDE information from the ultrasonic POD model. Such information could be used to quantify the risks associate with UT inspection or to select among different UT systems. Similar analysis capabilities will ultimately be available for other NDE methods, as well. Examples may be found in reports of current work in computer modeling of eddy current[12,13] and x-ray[14] flaw detection.

As an example of trade-off analysis, we will consider the following simulated inspection scenario. The components to be inspected are annular forgings of steel which may contain silicate inclusions. The inclusions are assumed to have mean orientations aligned with the forging flow lines with a possible random variability relative to that preferential alignment. The inclusions will be modeled as oblate spheroids; i.e., it is assumed that the forging pressures tend to flatten the inclusions. The material itself will be assumed to be homogeneous and isotropic; i.e., the material flow is assumed not to generate significant anisotropy. Inspection of the components will be by conventional gated peak detection of video signals relative to a standard calibrated, depth-dependent threshold amplitude. Inspection is assumed to be via a scanned immersion system. It is further assumed that accept/reject (A/R) decisions are based solely upon whether or not ultrasonic indications above the threshold are encountered. Specific inspection risk factors to be illustrated will include determination of minimum detectable flaw size (MDF) at a prepecified POD level, assessment of detection reliability (POD) of a prespecified critical defect size, and analysis of FA and FR type errors. Inspection system parameters considered in the simulations include probe frequency and focal length, orientation of the probe with respect to the part surface(s), scan plan characteristics, and specification of the threshold amplitude. Representative results of some of these simulations will be presented below.

An example of POD determination is illustrated in Fig. 1. This figure shows POD as a function of defect size (semi-major axis of a 4-1 oblate spheroidal inclusion) for several different mean defect orientations relative to the assumed 10 inch (25.4 cm) outside diameter (OD) of the forging. The defects were assumed to have a uniformly distributed random tilt and skew angle of +/- 5 degrees relative to their mean orientations. The inclusions were also assume to be uniformly randomly distributed throughout the component. The inspection was assumed to be a continuous rotational scan with a discrete index of 0.10 inches (0.254 cm) in the axial direction of the forging (i.e., a "drum" scan). The probe was tilted 7.2 degrees in an axial plane, corresponding to a refracted longitudinal wave angle of 30 degrees in the component. (Note that the mean tilt angles of the flaws are expressed relative to the refracted beam angle in Fig. 1; e.g. 0 degree tilt in the figure corresponds to a flaw oriented perpendicular to the beam). The

transducer was assumed to be a broad-band, planar probe with a nominal center frequency of 10 MHz. The detection threshold was assumed to be 100% of a #1 FBH oriented perpendicular to the beam and at the same depth below the OD as the inclusion.

As can be seen, the mean orientation of defects significantly affects their POD if this single probe orientation is used. This is, of course, not a surprising conclusion. In fact, inspection codes for forgings typically have specifications for beam propagation direction relative to flow line orientation. This model-based analysis, however, provides quantitative information about the degradation of detectability due to flow line orientation. This type of information could be used to specify an appropriate scan protocol required to achieve a predetermined detectability level (i.e., FA/FR rate, MDF, etc.). For example, assume that "adequate" detectability is defined by POD=0.90 for a presumed critical defect diameter (major axis of the spheroid) of 0.025 inch (0.064 cm). Then the inspection configuration used for Fig. 1 (i.e., 30 degree refracted L-wave, etc.) is "adequate" for flaws with a mean orientation perpendicular to the ultrasonic beam (the 0 degree curve in the figure). The configuration is only marginal if the flaws have a mean tilt of 7.5 degrees relative to the beam (i.e., from Fig. 1, POD=0.90 for a flaw size of 0.028 inch; POD=0.56 for the 0.025 inch flaw). Therefore, if all other inspection parameters are as described above, the refracted L-wave beam direction must be slightly less than 7.5 degrees from normal to the flaw in order that detectability be "adequate". Of course, to analyze this situation completely, more simulations for other refracted angles and defect orientations would need to be run. This information could be used to help select between an inexpensive scanner in which the probe angle must be set manually, thus requiring several scans of a component with different probe orientations, and a more expensive system in which the probe angle can be automatically varied during scanning. The trade-offs in that selection would involve, for example, weighing the purchase costs of each scanner against the inspection throughput rates.

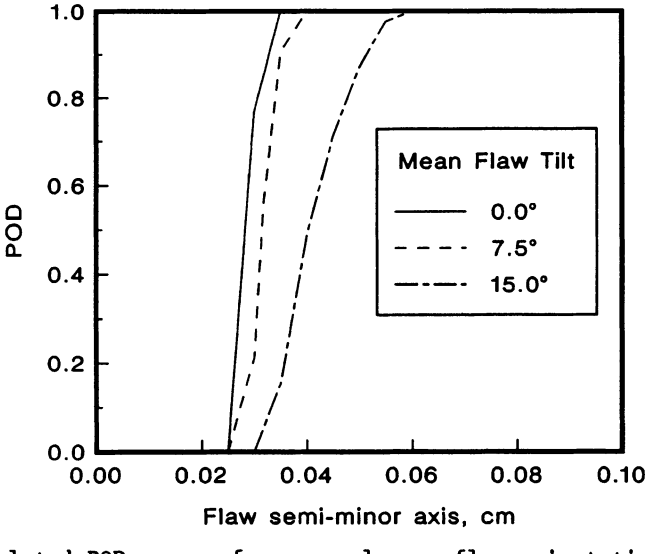

Fig. 1. Simulated POD curves for several mean flaw orientations. Angles are expressed relative to the UT beam axis (30 degree L-wave).

Next, we consider other inspection system parameters which affect detection reliability. For example, the threshold amplitude level can have a significant impact upon detectability. Figs. 2 and 3 show variation in POD for defects whose mean orientations are perpendicular and tilted 7.5 degrees, respectively, to the 30 degree refracted ultrasonic beam for three different threshold levels, which are expressed as percentages of the amplitude of a #1 FBH perpendicular to the beam. The other inspection parameters are the same as for the results in Fig. 1. As would be expected, lower threshold amplitudes yield higher POD values for a given defect size. However, lower threshold values also cause smaller defects to have significant POD. For example, from Fig. 2, the 50% threshold would cause components with 0.015 inch (.038 cm) diameter flaws with mean orientations normal to the beam to have a POD of 0.50. This would probably be an unacceptably high FR error based on the assumed 0.025 inch (0.64cm) critical defect size. There would be essentially zero FA error in this case, since POD=1.0 for defects of the critical size and larger. In contrast, the 100% threshold level in Fig. 2 exhibits a lower FR rate (e.g., POD=0.5 for a 0.023 inch flaw), but a higher FA since POD=0.9 at the critical flaw size (10% of critical defects would be passed). Similar results can be concluded from Fig. 3. Note that if the 85% threshold is selected, the critical defects can be adequately detected for mean flaw tilt angles up to 7.5 degrees from normal to the beam. This information would be useful for determining throughput rates of the less expensive scanner mentioned above, which could be inserted into a "cost model" for weighing the trade-offs described above.

Further analyses were performed for specification of scan plan parameters, which can also impact, among other things, the speed of inspection. Figs. 4 and 5 show the results of varying the scan index for a rotational scan through the OD of the forging. As before, the 30 degree refracted L-wave configuration was used and the flaws were assumed to have a mean orientation either normal or tilted 7.5 degrees to the beam. Results

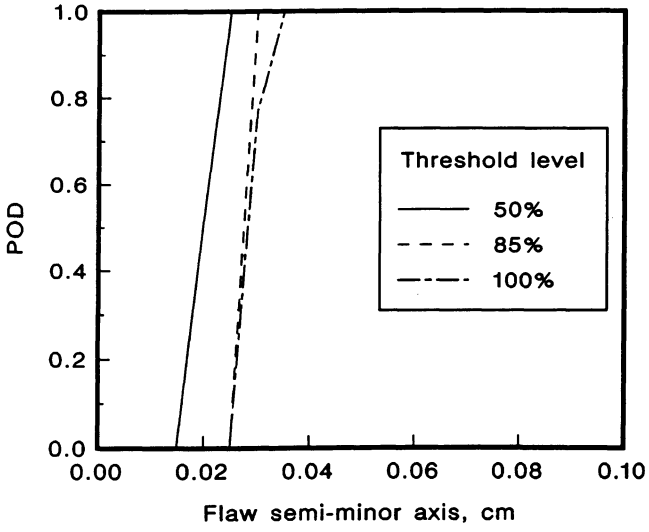

Fig. 2. Variation in POD for different detection thresholds for mean flaw orientations normal to the UT beam. Threshold levels are expressed as percentages of the amplitude of a #1 FBH normal to the beam.

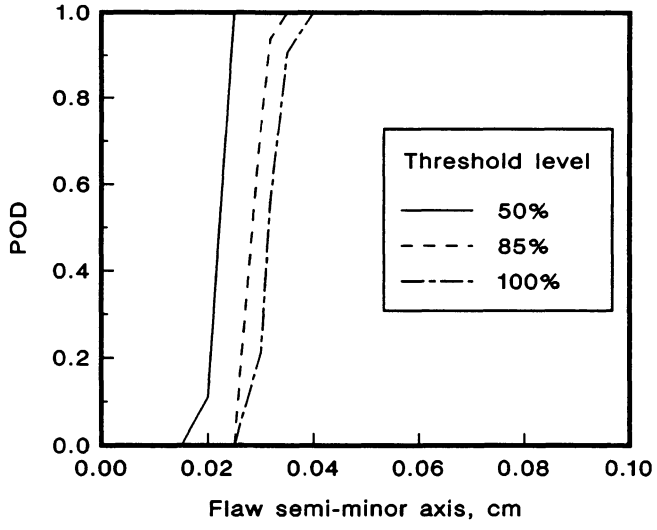

Fig. 3. Variation in POD for different detection thresholds for mean flaw tilt of 7.5 degrees relative to the UT beam. Threshold levels are expressed as percentages of the amplitude of a #1 FBH normal to the beam.

for three scan index values are illustrated. In addition, the threshold amplitude was chosen for each scan index value in such a way that POD=0.90 for roughly the same sized flaw at normal incidence to the beam. Therefore, the FA errors are essentially the same for the three scan index values shown in Fig. 4. (It is fortuitous that POD=0.90 for the same flaw size in each scan index case when the mean flaw tilt is 7.5 degrees, as shown in Fig. 5). Note that inspectability is "adequate", as defined above, for all cases in both figures. However, the 0.25 inch (0.635 cm) index shows a significantly higher FR error than the other two scan indices, which have nearly identical POD curves and, hence, FR rates for both flaw tilt angles.

SUMMARY

In this paper, we have described a model for predicting POD for defects in isotropic elastic components of complex geometrical shape and illustrated its use in analyzing the risks associated with the trade-offs among different NDE systems for inspecting a given component. The examples were chosen to illustrate the ability of the model to quantify the detection reliability variables, such as FA and FR errors, which must be considered to make effective decisions in selection of the best NDE system. As mentioned previously, such decisions must be based upon an "optimal" application of the NDE techniques to the inspection problem at hand. However, optimality is dependent upon factors other than detection reliability. For example, component cost, the possibility of loss of human life, cost of inspection hardware, inspection speed, operator skill levels, etc. must be incorporated into a "cost formula" appropriate to the problem. Since these factors are outside the realm of POD analysis, no attempt was made to formulate an optimization technique. Rather, we showed the ability of a model-based ultrasonic POD analysis package, which explicitly incorporates parameters describing the inspection system, the component design, and the critical defects, to simulate the variability of defect detectability as a function of those parameters. This approach will be of great benefit in the selection

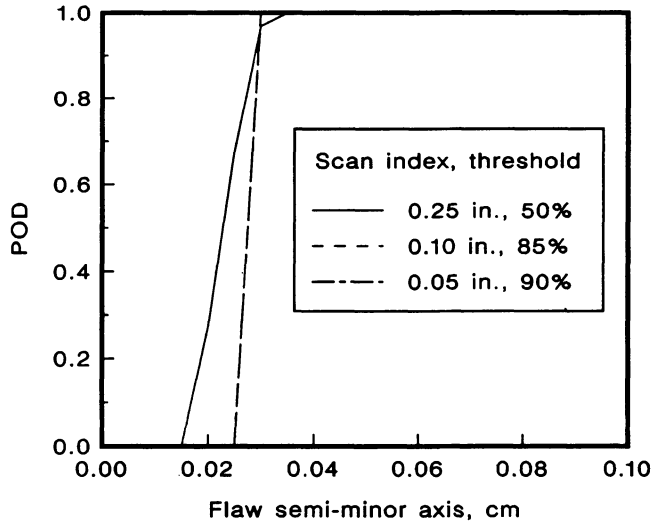

Fig. 4. Variation of POD of defects with mean orientations normal to the UT beam for different scan index values. Thresholds are expressed as a percentage of the amplitude of a #1 FBH normal to the beam.

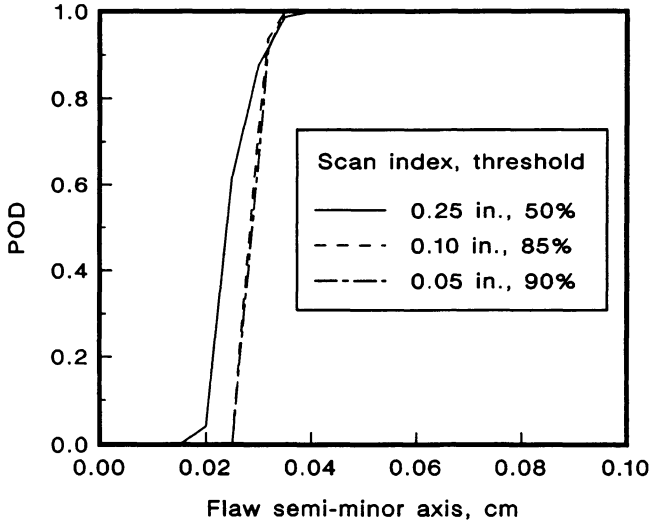

Fig. 5. Variation of POD of defects with a mean tilt of 7.5 degrees relative to the UT beam for different scan index values. Thresholds are expressed as a percentage of the amplitude of a #1 FBH normal to the UT beam.

among different NDE approaches when similar modeling capabilities become available for the other inspection modalities. In addition, since the design parameters of a component can be varied at will, these models can also be used to investigate the effects of design modifications upon defect detectability and, hence, be useful tools for integration into computer-aided-design.

ACKNOWLEDGEMENT

This work was supported by the Center for NDE at Iowa State University and was performed at the Ames Laboratory. The Ames Laboratory is operated for the U.S. Department of Energy by Iowa State University under Contract W-7405-ENG-82.

REFERENCES

1. H. M. Burte and D. E. Chimenti, in Review of Progress in Quantitative NDE, vol. 6B, D. O. Thompson and D. E. Chimenti, eds., Plenum Press, New York, 1987, pp. 1797-1809.
2. R. B. Thompson and T. A. Gray, J. Acoust. Soc. Am. 74(4), 1983, pp. 1279-1290.
3. T. A. Gray, R. B. Thompson and B. P. Newberry, in Review of Progress in Quantitative NDE, vol. 4A, D. O. Thompson and D. E. Chimenti, eds., Plenum Press, New York, 1985, pp. 11-17.
4. R. B. Thompson and T. A. Gray, Phil. Trans. R. Soc. Lond. A 320, 1986, pp. 329-340.
5. T. A. Gray and R. B. Thompson, in Review of Progress in Quantitative NDE, vol. 5A, D. O. Thompson and D. E. Chimenti, eds., Plenum Press, New York, 1986, pp. 911-918.
6. B. A. Auld, Wave Motion 1, 1979, pp. 3-10.
7. T. A. Gray, R. B. Thompson, and B. P. Newberry, in Review of Progress in Quantitative NDE, vol. 6A, D. O. Thompson and D. E. Chimenti, eds., Plenum Press, New York, 1987, pp. 957-965.
8. M. Schwartz, Information Transmission, Modulation and Noise, 2nd. ed., McGraw-Hill, New York, 1970, pp. 361-372, 444-451.
9. See e.g., J.-S. Chen and L. W. Schmerr, these proceedings.
10. J. L. Opsal and W. M. Visscher, J. Appl. Phys. 58(3), 1985, pp. 1102-1115.
11. R. B. Thompson and T. A. Gray, in Review of Progress in Quantitative NDE, vol. 1, D. O. Thompson and D. E. Chimenti, eds., Plenum Press, New York, 1982, pp. 233-249.
12. N. Nakagawa and V. G. Kogan, these proceedings.
13. R. E. Beissner, these proceedings.
14. J. N. Gray, these proceedings.